Cell Reports

A 5,000-year-old hunter-gatherer already plagued by *Yersinia pestis*

Graphical abstract

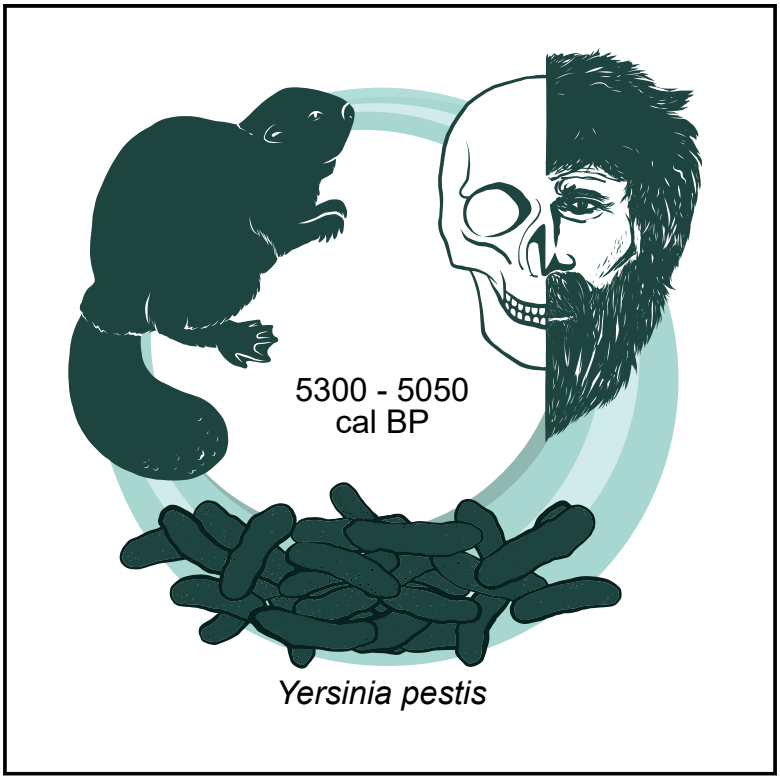

Highlights

- *Yersinia pestis* is discovered in a 5,000-year-old hunter-gatherer from Latvia
- *Y. pestis* emerged ~7,000 years ago at the beginning of the Neolithic
- The infected individual might represent a case of septicemic plague due to zoonosis

Authors

Julian Susat, Harald Lübke, Alexander Immel, ..., Valdis Bērziņš, Almut Nebel, Ben Krause-Kyora

Correspondence

b.krause-kyora@ikmb.uni-kiel.de

In brief

Susat et al. reconstruct the genome of a 5,000-year-old *Yersinia pestis* strain detected in a hunter-gatherer from Latvia. The results show that the basal lineages evolved already at the beginning of the Neolithic and had presumably limited infection potential, suggesting isolated zoonotic events as causative triggers.

Susat et al., 2021, Cell Reports *35*, 109278
June 29, 2021 © 2021 The Author(s).
https://doi.org/10.1016/j.celrep.2021.109278

CellPress

Cell Reports

CellPress
OPEN ACCESS

Report

A 5,000-year-old hunter-gatherer already plagued by *Yersinia pestis*

Julian Susat,[1,11] Harald Lübke,[2,11] Alexander Immel,[1] Ute Brinker,[2] Aija Macāne,[3] John Meadows,[2,4] Britta Steer,[5] Andreas Tholey,[5] Ilga Zagorska,[6] Guntis Gerhards,[6] Ulrich Schmölcke,[2] Mārcis Kalniņš,[6] Andre Franke,[1] Elīna Pētersone-Gordina,[6] Barbara Teßman,[7] Mari Tõrv,[8] Stefan Schreiber,[1,9] Christian Andree,[10] Valdis Bērziņš,[6] Almut Nebel,[1] and Ben Krause-Kyora[1,12,*]

[1]Institute of Clinical Molecular Biology, Kiel University, Rosalind-Franklin-Str. 12, 24105 Kiel, Germany
[2]Centre for Baltic and Scandinavian Archaeology (ZBSA), Schleswig-Holstein State Museums Foundation Schloss Gottorf, Schlossinsel 1, 24837 Schleswig, Germany
[3]Department of Historical Studies, University of Gothenburg, PO Box 200, SE405 30 Göteborg, Sweden
[4]Leibniz Laboratory for AMS Dating and Isotope Research, Kiel University, Max-Eyth-Str. 11-13, 24118 Kiel, Germany
[5]Systematic Proteomics & Bioanalytics, Institute for Experimental Medicine, Kiel University, Niemannsweg 11, 24105 Kiel, Germany
[6]Institute of Latvian History, University of Latvia, Kalpaka bulv. 4, 1050 Riga, Latvia
[7]Berlin Society of Anthropology, Ethnology and Prehistory, c/o Museum of Pre- and Protohistory, Geschwister-Scholl-Str. 6, 10117 Berlin, Germany
[8]Department of Archaeology, Institute of History and Archaeology, University of Tartu, Jakobi 2, 51005 Tartu, Estonia
[9]Department of General Internal Medicine, University Hospital Schleswig-Holstein, Kiel University, Rosalind-Franklin-Str. 12, 24105 Kiel, Germany
[10]Research Center of Medical History, Kiel University, Breiter Weg 10, 24105 Kiel, Germany
[11]These authors contributed equally
[12]Lead contact
*Correspondence: b.krause-kyora@ikmb.uni-kiel.de
https://doi.org/10.1016/j.celrep.2021.109278

SUMMARY

A 5,000-year-old *Yersinia pestis* genome (RV 2039) is reconstructed from a hunter-fisher-gatherer (5300–5050 cal BP) buried at Riņņukalns, Latvia. RV 2039 is the first in a series of ancient strains that evolved shortly after the split of *Y. pestis* from its antecessor *Y. pseudotuberculosis* ~7,000 years ago. The genomic and phylogenetic characteristics of RV 2039 are consistent with the hypothesis that this very early *Y. pestis* form was most likely less transmissible and maybe even less virulent than later strains. Our data do not support the scenario of a prehistoric pneumonic plague pandemic, as suggested previously for the Neolithic decline. The geographical and temporal distribution of the few prehistoric *Y. pestis* cases reported so far is more in agreement with single zoonotic events.

INTRODUCTION

The archaeological shell midden site of Riņņukalns is located in Latvia, next to the River Salaca, which flows into the Baltic Sea (Figure 1A). The shell midden itself consists of alternating layers of unburnt freshwater mussel shells, burnt mussel shells, and fish bones that were deposited by human activity in a short period of 100–200 years in the early 6th millennium before present (BP) (Bērziņš et al., 2014; Brinker et al., 2020). In 1875, amateur archaeologist Carl Georg Count Sievers (1814–1879) conducted the first systematic excavation of Riņņukalns. Sievers detected in two single graves the skeletal remains of a 12- to 18-year-old woman (RV 1852) and a 20- to 30-year-old man (RV 2039; Figures 1B and 1C; Table 1), covered by intact midden layers. Due to the stratigraphic position, he assumed a prehistoric context of these burials (Sievers, 1875). This interpretation was considered wrong at the time and therefore met with fierce resistance (Grewingk, 1878; Brinker et al., 2018). For confirmation of his hypothesis and osteological investigations, Sievers sent the crania of the specimens RV 1852 and RV 2039, among other human remains from Riņņukalns, to his future mentor and friend, the already world-famous German physician Rudolf Virchow (1821–1902) in Berlin (Virchow, 1877). Virchow is still highly renowned for establishing the fields of cellular pathology, the basis of modern medicine, and social medicine. In 1869, because of his avid interest in pre- and protohistory, he became the founder of the Berlin Society of Anthropology (today known as Berliner Gesellschaft für Anthropologie, Ethnologie und Urgeschichte [BGAEU]) (Andree, 1976). Despite his worldwide reputation, Virchow lent amateur researchers such as Heinrich Schliemann and Sievers his expertise for their archaeological projects without being deterred by the opposing views of his contemporaries. After being convinced by Sievers of the importance of his finds, Virchow examined the complete Riņņukalns material and published a first report (Brinker et al., 2018; Virchow, 1877). After World War II, the Riņņukalns crania seemed

This is an open access article under the CC BY license (http://creativecommons.org/licenses/by/4.0/).

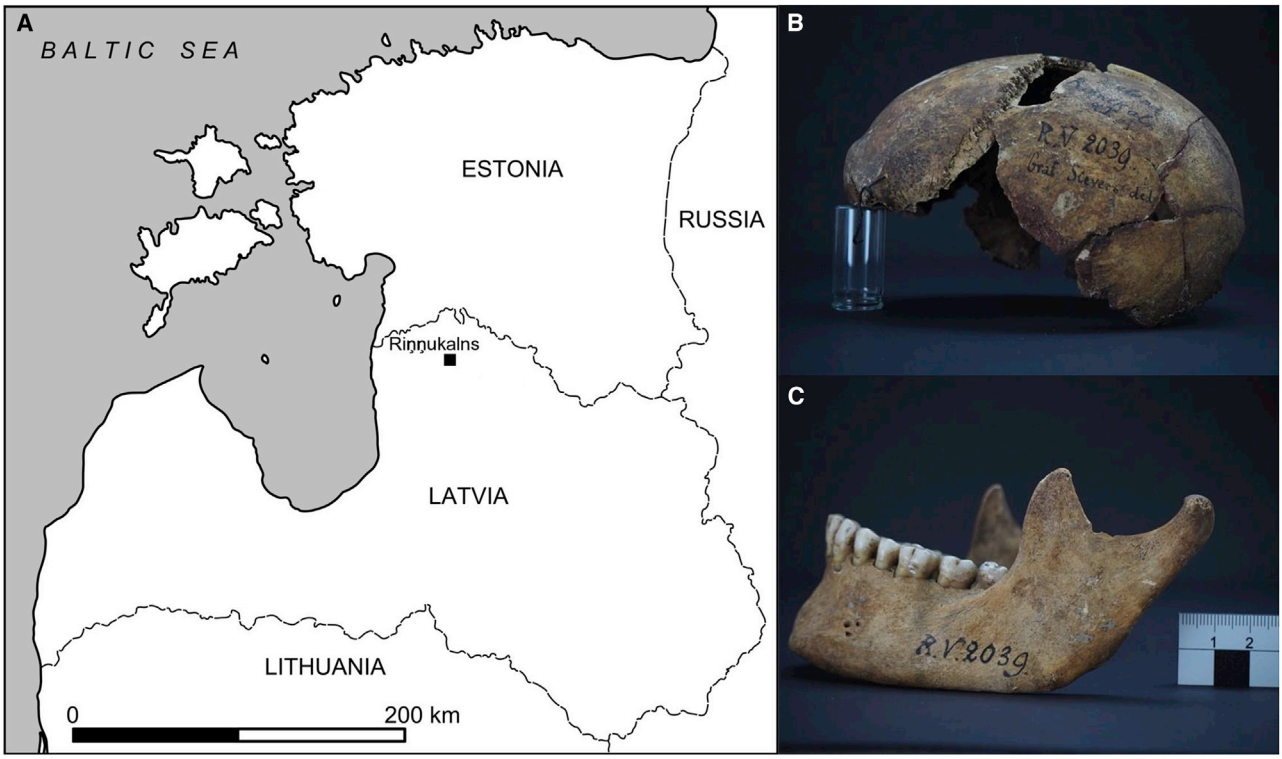

Figure 1. Site Riņņukalns

(A) Map with the site Riņņukalns from where the individuals presented in this study were recovered.

(B and C) Cranium (B) and mandible (C) of individual RV 2039 rediscovered in the Anthropological Rudolf Virchow Collection of the Berlin Society of Anthropology, Ethnology and Prehistory (Berliner Gesellschaft für Anthropologie, Ethnologie und Urgeschichte [BGAEU]).

to have disappeared and their whereabouts were deemed unknown, but in 2011, the skulls were rediscovered in the re-inventoried Anthropological Rudolf Virchow Collection of the BGAEU, where they had apparently been kept (Lübke et al., 2016). Concurrent with the search for the crania, new field work on the Riņņukalns site led to the detection of two additional burials, those of an adult male (2017/1) and a neonate (2018/1) (Table 1; Brinker et al., 2020). Also, for these skeletal remains, the archaeological stratigraphy indicated a prehistoric origin. All four specimens, including RV 1852 and RV 2039 from the Virchow Collection, were subsequently radiocarbon dated to 5300–5050 cal (calibrated years) BP, thus confirming Sievers' original assessment (Brinker et al., 2020). The individuals buried in the midden belonged to a group of complex hunter-fisher-gatherers (Ames, 2014). They most probably lived in semi-permanent or permanent settlements on the banks of the River Salaca. The valuable aquatic food resources certainly provided enough food for year-round habitation (Brinker et al., 2020).

Because not much is known about the genomic composition of hunter-gatherers who lived in northeastern Europe 5,000 years ago or about their infectious disease burden, we subjected the four Riņņukalns individuals to an ancient DNA (aDNA) analysis that also included a pathogen screening. Surprisingly, in one male, we identified the genome of *Yersinia pestis*, the infectious agent responsible for at least three historical plague epidemics (Wagner et al., 2014). Our finding presents evidence of this bacterium in a hunter-gatherer and sheds more light on the very early phases of *Y. pestis* evolution and diversification.

RESULTS

We generated genome-wide shotgun sequences from various skeletal elements (teeth, petrous bones) of the four Riņņukalns individuals (Table 1). We screened the datasets for the presence of known bacterial and viral pathogens by using an established in-house pipeline (Krause-Kyora et al., 2018a, 2018b; Susat et al., 2020). In sample RV 2039 (Figure 1; dated to 5300–5050 cal BP), we observed *Y. pestis*-specific reads that showed typical aDNA damage patterns and length distributions, thus supporting the ancient origin of the sequences (Table 1). The other extracts did not yield signs of *Y. pestis*. For RV 2039, we reconstructed the *Y. pestis* genome (i.e., chromosome, plasmids pCD1 and pPCP1) at high coverage (Table 1). The plasmid pMT1 lacked a 20-kb region containing the virulence factor *ymt*; this characteristic was reported previously for other ancient *Y. pestis* strains (Andrades Valtueña et al., 2017). Phylogenetic analysis with 278 genomes (including RV 2039, 276 previously published ancient and modern *Y. pestis* genomes, and one *Y. pseudotuberculosis* genome; Table S1) placed RV 2039 basal to all known *Y. pestis* bacteria (Figure 2). The Riņņukalns strain had its own clade and marked the first branching event after the split from the bacterium *Y. pseudotuberculosis*. RV 2039

Table 1. Overview of samples and mapping results

Human genome (hg19)

Sample	Material	Generated reads in mill. (raw reads)	Clipped and merged reads in mill.	Reads mapped against hg19 in mill.	Damage 1st base 5′, %	Damage 1st base 3′, %	No. SNPs from the 1,240K panel	Osteological sex	Age at death	Genetic sex	Mt haplo type	Y haplo type
RV 1852	petrous bone/ tooth	74.7	39.9	25.4	4.4	4.1	236,243	female	12–18 years	female	U5a1d1	–
RV 2039	tooth	3,160	1,650	84.4	4.7	4.1	394,544	male	20–30 years	male	U5a2b2	BT
2017/01	petrous bone/ tooth	20.2	11.4	6.6	7.9	6.8	77,798	male	35–45 years	male	U4a1	K
2018/1	petrous bone	2.9	1.4	1.0	7.9	7.3	11,509	–	38–40 prenatal weeks	male	U5a1d1	CT

Y. pestis, sample RV 2039

Reference	Aligned reads	Coverage ≥1×, %	Coverage ≥2×, %	Coverage ≥3×, %	Mean coverage whole reference	Damage 1st base 5′, %	Damage 1st base 3′, %
chromosome NC_003143.1	600,065	92.39	86.75	78.29	5.85×	7.2	7.1
pMT1 NC_003134.1	2,144	46.62	21.28	8.88	0.83×	6.8	6.3
pPCP1 NC_003132.1	1,050	78.05	72.24	66.14	5.10×	9.9	12.9
pCD1 NC_003131.1	18,005	92.04	90.31	87.88	12.00×	10.3	10.2

was clearly separated from all later-dating Neolithic and Bronze Age strains (Figure 3). A TempEst analysis based on 42 selected genomes, including RV 2039, indicated a temporal signal in the molecular phylogeny (Figure S1). To estimate divergence times, we performed molecular clock analyses by using BEAST2 with two independent runs. The first run is based on a rooted starting tree, which BEAST2 is allowed to alter; in the second run, no starting tree was provided (Figures 3 and S2). The results of both analyses were congruent and showed that RV 2039 diverged from all other *Y. pestis* bacteria ~7100 cal BP (with starting tree, 8693–5669 cal BP; without starting tree, 8895–5733 cal BP). The split between *Y. pestis* and *Y. pseudotuberculosis* was dated to ~7400 cal BP (with starting tree, 9069–5782 cal BP; without starting tree, 9223–5833 cal BP).

Investigation of the genomic structure of RV 2039 led to the discovery of 106 exclusive SNPs that are not known to have an effect on virulence factors (Table S2). Apart from the *ymt* gene, whose absence is specific for the Neolithic/Bronze Age clade, no other virulence factor was missing. The virulence-associated genes *ureD*, *flhD*, and *pde2* and the plasminogen activator *pla* exhibited the ancestral states, as already shown for the Neolithic and Bronze Age lineages (Andrades Valtueña et al., 2017; Demeure et al., 2019). The results of the genomic and phylogenetic analyses were supported by the archaeological age of RV 2039, rendering it as one of the earliest lineages in *Y. pestis* evolution.

To confirm the presence of *Y. pestis* in RV 2039 at the protein level, we performed a liquid chromatography-mass spectrometry (LC-MS)-based proteomics analysis. We identified three different peptides from three proteins that are specific for *Y. pestis* (Figure S3), together with ~118 human proteins.

The human endogenous DNA content in the four datasets was sufficient to perform kinship and population genomic analyses in the four Riņņukalns individuals (Table 1). Kinship analysis did not provide evidence of relatedness among the four individuals buried in the shell midden. All four carried a large genomic ancestry component that is specific for hunter-gatherers. In particular, they had a high affinity to hunter-gatherers of eastern Europe (Figure S4), who inhabited a large area stretching from the Baltic Sea to the Pontic-Caspian steppe (Mathieson et al., 2018).

DISCUSSION

We reconstructed a 5,000-year-old *Y. pestis* genome (RV 2039) from the remains of an adult man (dated to 5300–5050 cal BP) who was buried in the shell midden of Riņņukalns, Latvia. This diagnosis was confirmed independently by the detection of three *Y. pestis*-specific proteins in the sample. RV 2039 is basal to all known ancient or modern *Y. pestis* bacteria. It represents a very early, independent lineage that emerged ~7,000 years ago, only a few hundred years after the split of the *Y. pestis* clade from its antecessor *Y. pseudotuberculosis*. Our date of 7400 cal BP for this split is ~1,000 years earlier than the previously reported estimates (Andrades Valtueña et al., 2017; Demeure et al., 2019; Rascovan et al., 2019; Rasmussen et al., 2015; Spyrou et al., 2018). The subsequent large-scale branching and geographic radiation of *Y. pestis* occurred between 7,000 and 5,000 years ago (Andrades Valtueña et al., 2017; Demeure et al., 2019; Rascovan et al., 2019; Rasmussen et al., 2015; Spyrou et al., 2018). This time range coincides with the beginning of the Neolithic

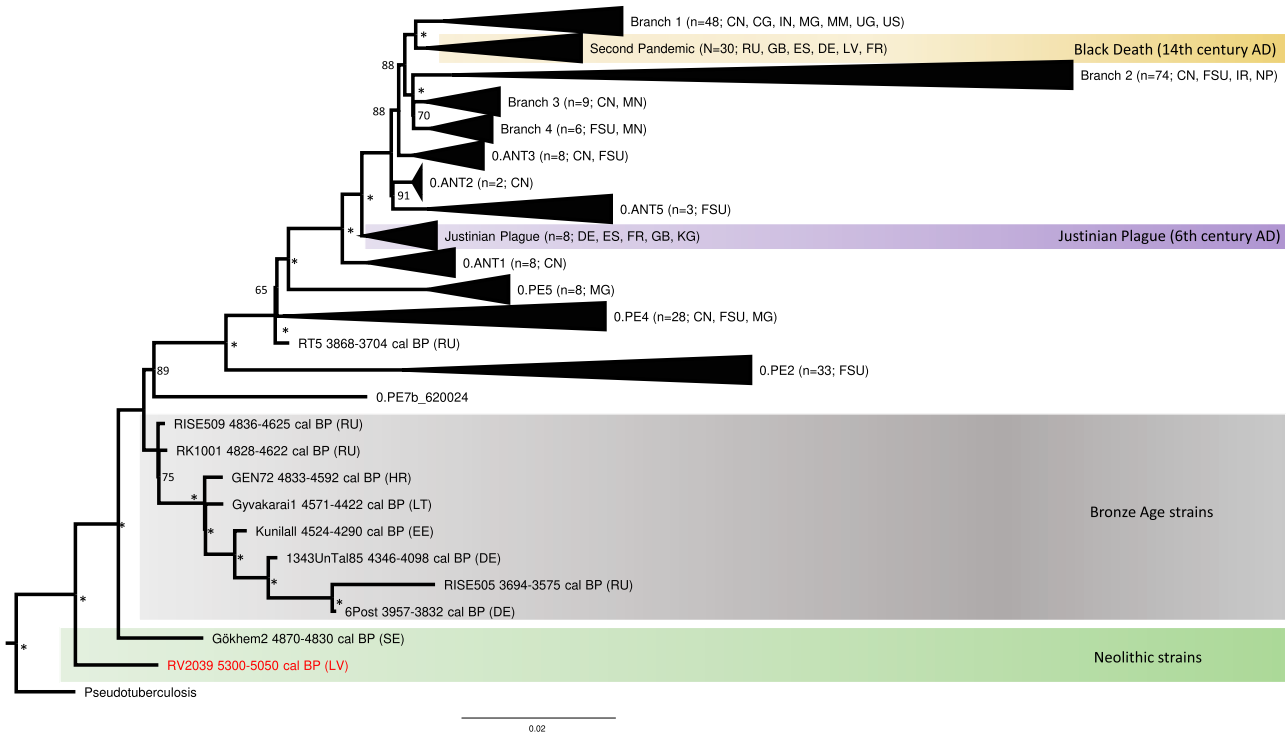

Figure 2. Maximum likelihood tree

The tree is based on the SNP alignment (18,169 positions) of 228 modern *Y. pestis* genomes, 48 published ancient *Y. pestis* strains, 1 *Y. pseudotuberculosis* genome, and the strain from Riņņukalns (RV 2039 in red). Country abbreviation is given in parentheses (DE, Germany; ES, Spain; FR, France; GB, Great Britain; US, United States; RU, Russia; LV, Latvia; CN, China; CG, Congo; FSU, Former Soviet Union; IN, India; IR, Iran; MG, Madagascar; MM, Myanmar; MN, Mongolia; NP, Nepal; UG, Uganda; KG, Kyrgyzstan; CH, Switzerland; HR, Croatia; EE, Estonia; LT, Lithuania; SE = Sweden). Neolithic strains are highlighted in green, Bronze Age strains in gray, strains from the Justinian Plague in purple, and strains from the Black Death in yellow. Bootstrap values are shown on the nodes for 500 replicates, and an asterisk (*) represents a bootstrap support above 95.

period in Europe (~7500–5000 cal BP) rather than with its decline, as suggested previously (Rascovan et al., 2019).

RV 2039 marks the beginning of *Y. pestis* evolution and is the first in a series of ancient strains that eventually became extinct. RV 2039 and its slightly younger relative, the Gok2 genome from a Neolithic farmer in Sweden (dated to 5040–4867 cal BP), are on separate branches and both are distinct from later-dating Neolithic and Bronze Age strains (Rascovan et al., 2019). Apart from RV 2039 and Gok2, four more very early *Y. pestis* genomes have been identified in human remains from Estonia, Lithuania, and Sweden, reflecting a noteworthy accumulation of *Y. pestis*-positive finds in northeastern Europe (Andrades Valtueña et al., 2017; Rascovan et al., 2019; Rasmussen et al., 2015; Spyrou et al., 2018).

Archaeological and isotope evidence clearly showed that the infected individual from Riņņukalns followed a lifestyle and diet (based on freshwater resources) that are typically associated with hunter-gatherers of the Baltic region at that time (Meadows et al., 2018). The human genomic data support this cultural affiliation and indicate a strong link with eastern hunter-gatherers that roamed the forest steppe zone between the Black and Baltic seas during the 6th millennium cal BP (Mathieson et al., 2018). Riņņukalns' "gateway" location and archaeological artifacts show that the site was an integral part of a long-distance exchange via the river networks of the East European Plain (Loze, 2001; Núñez and Franzén, 2011; Kriiska, 2015). Such an exchange system was evidently maintained through intensive and regular contacts between human groups.

Modern *Y. pestis* can be transmitted from animals (e.g., rodents) to humans (Demeure et al., 2019). It is possible that hunter-gatherers, who frequently killed rodents for food or personal decoration, contracted *Y. pestis* or its antecessor *Y. pseudotuberculosis* directly from animals. Interestingly, at the Riņņukalns site, beaver (*Castor fiber*) was the most frequently recorded species among the archaeozoological finds excavated by Sievers (Rütimeyer, 1877). Beavers are a common carrier of *Y. pseudotuberculosis*, which directly precedes our early *Y. pestis* strain (Gaydos et al., 2009). Despite this interesting observation, it remains unknown to what degree hunter-gatherers may have played a role in the zoonotic emergence, early evolution, or spread of *Y. pestis.*

Although the hunter-gatherer from Riņņukalns was infected with *Y. pestis*, it is not clear whether or to what extent he was actually affected by the plague. RV 2039 did not yet have the genetic components for flea adaptation needed to transmit the bacterium efficiently to the human host (bubonic plague). However, the genomic data suggest that it was theoretically capable of spreading to the lungs (pneumonic plague) and of infecting

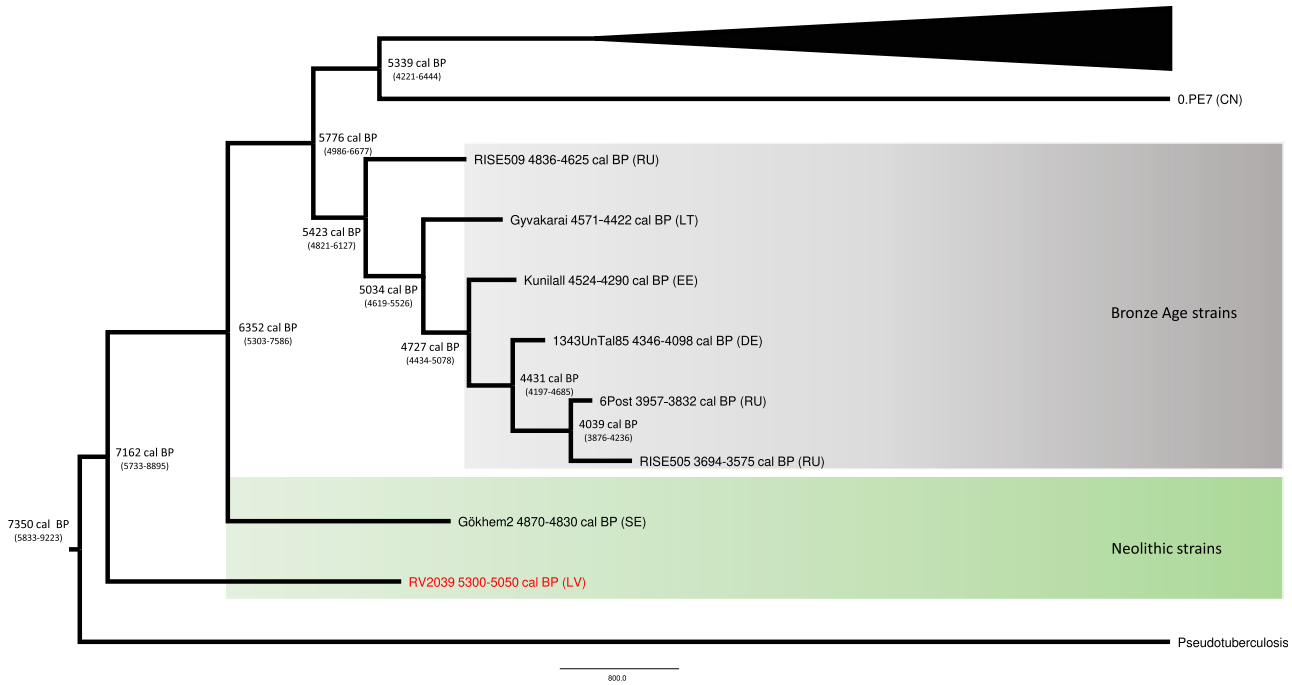

Figure 3. Molecular clock estimation (without starting tree) of modern and ancient Y. *pestis* strains

BEAST2 maximum clade credibility tree based on 41 modern and ancient Y. *pestis* genomes and the strain from Riņņukalns (RV 2039 in red). The final tree was summarized from 900 million states and 810,252 trees showing the mean divergence dates as tree nodes and the range for the dating in brackets. Country abbreviation is given in parentheses (DE, Germany; RU, Russia; LV, Latvia; CN, China; EE, Estonia; LT, Lithuania; SE = Sweden). Neolithic strains are highlighted in green and Bronze Age strains in gray.

other hosts via droplets. However, the pneumonic plague is rare today and was also most likely rare in the past. In addition, the absence of the I259T mutation in the *pla* gene may have compromised the dissemination capabilities of RV 2039, allowing only localized outbreaks of pneumonic plague (Zimbler et al., 2015). RV 2039 could also have been transmitted directly via a bite from a rodent or a carnivore, leading to septicemic plague that is usually restricted to the infected individual. Also, with regard to other virulence factors, RV 2039 consistently showed the ancestral alleles typical of *Y. pseudotuberculosis*, an enteric bacterium that is also known to cause disease (Bertelli et al., 2014). RV 2039 shared many of its ancestral characteristics with the other Neolithic/Bronze Age strains. It was only millennia later (~3800 cal BP) that *Y. pestis* had acquired all of the mutations for flea-based transmission (Demeure et al., 2019). This step is considered crucial in *Y. pestis* evolution because it required the death of the host to ensure perpetuation of the bacterium via the flea vector (Brubaker, 1991). Thus, subsequent selective pressures facilitated mechanisms promoting the invasion of human tissues, bacteremia, and lethality that turned the bubonic plague into a highly deadly disease (Brubaker, 1991).

Interestingly, in the RV 2039 dataset, the *Y. pestis*-specific reads were very frequent, although they had been generated by shotgun sequencing without any prior enrichment. Many of the other prehistoric *Y. pestis* genomes were also assembled with only shotgun data (Andrades Valtueña et al., 2017; Rascovan et al., 2019; Rasmussen et al., 2015; Spyrou et al., 2018). The abundance of *Y. pestis* reads in the aDNA extracts suggests a high bacterial load in the bloodstreams of the diseased at the time of death. Remarkably, infection experiments with different *Yersinia* species in mice have shown a negative correlation between the number of bacteria during the terminal stage and their virulence (Brubaker, 1991). It is tempting to hypothesize that this correlation also holds for the different ancient *Y. pestis* strains. If true, prehistoric strains with a high bacterial load may have had a lower virulence. However, this does not mean that these strains were harmless. Given their presence in the blood of the infected, they could still have been potentially deadly for the individual.

Admittedly, so far there is no experimental information available about the pathogenicity of the ancient *Y. pestis* strains. Therefore, it is difficult to assess their ability to cause a disease of epidemic proportions. The possible consequences of an infection for a population in terms of disease burden are still unknown. However, based on the genomic data, it cannot be excluded that RV 2039 and the other early forms were less transmissible than the later strains, leading only to local outbreaks (Zimbler et al., 2015). In this context, it is interesting to note that almost all infected prehistoric individuals (apart from Gok2) represented sporadic cases and were regularly interred in single or multiple burials. Also, the man from Riņņukalns was carefully buried, as were the other three contemporaneous individuals in whom we did not find any evidence of *Y. pestis*. These findings argue against an infestation of the whole group with a bacterium that kills its hosts within a few days, as would be expected for the pneumonic plague. Thus, it is conceivable that

the *Y. pestis*-positive individual contracted the bacterium via an animal bite (zoonosis), resulting in the septicemic form of plague. At this stage it seems premature to associate the presence of early *Y. pestis* genomes in roughly a dozen human skeletons across the vast Eurasian continent and over a period of about 2 millennia with a prehistoric pneumonic plague pandemic, as has been done recently (Rascovan et al., 2019). Such a distribution pattern appears more consistent with the scenario of isolated zoonotic events in sparsely populated areas.

Our study shows the power of modern aDNA sequencing technology to detect ancient pathogens, especially bacteria such as *Y. pestis* that do not leave telltale lesions on bone. With the scientific toolkit available at the time, Virchow was in no position to diagnose the plague on the Riņņukalns cranium. However, thanks to Virchow's progressive scientific approach, the remains excavated by Sievers were stored in his collection, where they survived the vicissitudes of time unscathed, so that a later diagnosis was still possible, even after 145 years.

STAR★METHODS

Detailed methods are provided in the online version of this paper and include the following:

- KEY RESOURCES TABLE
- RESOURCE AVAILABILITY
  - Lead contact
  - Materials availability
  - Data and code availability
- EXPERIMENTAL MODEL AND SUBJECT DETAILS
  - Anthropological Rudolf Virchow Collection
- METHOD DETAILS
  - Anthropological analysis
  - aDNA extraction and sequencing
  - *Yersinia pestis* genetic analyses
  - Molecular dating
  - SNP effect and analysis of virulence factors
  - Human population genetic analyses
  - Proteomic analysis

SUPPLEMENTAL INFORMATION

Supplemental information can be found online at https://doi.org/10.1016/j.celrep.2021.109278.

ACKNOWLEDGMENTS

This study was funded by the Deutsche Forschungsgemeinschaft (DFG, German Research Foundation) project no. 290391021 – CRC 1266 and under Germany's Excellence Strategy EXC 2167–390884018 and EXC 2150–390870439. The anthropological and archaeological research on Riņņukalns is part of the project "Riņņukalns, ein neolithischer Süsswassermuschelhaufen im Norden Lettlands und seine Bedeutung für die steinzeitliche Kulturentwicklung im östlichen Baltikum" funded by the DFG (project no. 335674082) and of the project of the University of Latvia "Letonica, Diaspora and Intercultural Communication" (ZD2015/AZ85). We thank the Berlin Society of Anthropology, Ethnology and Prehistory for the opportunity to re-examine the skulls and take the necessary samples for the analyses.

AUTHOR CONTRIBUTIONS

B.K.-K., H.L., and V.B. developed the idea for this study. A.M., I.Z., G.G., M.K., E.P.-G., B.T., and M.T. provided the human skeletal remains. U.B., B.T., M.T., G.G., E.P.-G., and J.M. analyzed and dated the human remains. B.K.-K. and A.F. generated the aDNA data. J.S., A.I., and B.K.-K. analyzed the aDNA data. A.T. and B.S. analyzed the ancient protein data. A.N., J.S., C.A., H.L., U.S., I.Z., V.B., S.Sch., and B.K.-K. interpreted the findings. A.N., J.S., H.L., and B.K.-K. wrote the manuscript with input from all of the other authors.

DECLARATION OF INTERESTS

The authors declare no competing interests.

Received: September 21, 2020
Revised: December 18, 2020
Accepted: May 28, 2021
Published: June 29, 2021

REFERENCES

Ames, K.M. (2014). Complex Hunter-Gatherers. In Encyclopedia of Global Archaeology, C. Smith, ed. (Springer), pp. 1613–1621.

Andrades Valtueña, A., Mittnik, A., Key, F.M., Haak, W., Allmäe, R., Belinskij, A., Daubaras, M., Feldman, M., Jankauskas, R., Janković, I., et al. (2017). The Stone Age Plague and Its Persistence in Eurasia. Curr. Biol. *27*, 3683–3691.e8.

Andree, C. (1976). Rudolf Virchow als Prähistoriker (Böhlau Verlag).

Bertelli, L., Masetti, R., Bardasi, G., Maretti, M., Gargano, T., Corsini, I., Melchionda, F., Tassinari, D., Cazzato, S., Lima, M., and Pession, A. (2014). Two cases of abdominal pain in children with mesenteric lymphadenitis due to Yersinia pseudotuberculosis infection. J. Pediatr. *165*, 411–411.e1.

Bērziņš, V., Brinker, U., Klein, C., Lübke, H., Meadows, J., Rudzite, M., Schmölcke, U., Stümpel, H., and Zagorska, I. (2014). New research at Rinnukalns, a Neolithic freshwater shell midden in northern Latvia. Antiquity *88*, 715–732.

Bos, K.I., Schuenemann, V.J., Golding, G.B., Burbano, H.A., Waglechner, N., Coombes, B.K., McPhee, J.B., DeWitte, S.N., Meyer, M., Schmedes, S., et al. (2011). A draft genome of Yersinia pestis from victims of the Black Death. Nature *478*, 506–510.

Bos, K.I., Harkins, K.M., Herbig, A., Coscolla, M., Weber, N., Comas, I., Forrest, S.A., Bryant, J.M., Harris, S.R., Schuenemann, V.J., et al. (2014). Pre-Columbian mycobacterial genomes reveal seals as a source of New World human tuberculosis. Nature *514*, 494–497.

Bos, K.I., Herbig, A., Sahl, J., Waglechner, N., Fourment, M., Forrest, S.A., Klunk, J., Schuenemann, V.J., Poinar, D., Kuch, M., et al. (2016). Eighteenth century Yersinia pestis genomes reveal the long-term persistence of an historical plague focus. eLife *5*, e12994.

Bouckaert, R., Vaughan, T.G., Barido-Sottani, J., Duchêne, S., Fourment, M., Gavryushkina, A., Heled, J., Jones, G., Kühnert, D., De Maio, N., et al. (2019). BEAST 2.5: An advanced software platform for Bayesian evolutionary analysis. PLoS Comput. Biol. *15*, e1006650.

Brinker, U., Bērziņš, V., Ceriņa, A., Gerhards, G., Kalniņš, M., Krause-Kyora, B., Lübke, H., Meadows, J., Meinel, D., Ritchie, K., et al. (2020). Two burials in a unique freshwater shell midden: insights into transformations of Stone Age hunter-fisher daily life in Latvia. Archaeol. Anthropol. Sci. *12*, 97.

Brinker, U., Meinel, D., Teßmann, B., and Lübke, H. (2018). Die menschlichen Skelettreste der zur anthropologischen Rudolf-Virchow-Sammlung gehörenden Kollektion des Fundplatzes Riņņukalns im Norden Lettlands – Resultat eines Forschungsstreites des 19. Jahrhunderts im damaligen Livland. Mitteilungen der Berliner Gesellschaft für Anthropologie, Ethnologie und Urgeschichte *39*, 35–54.

Brubaker, R.R. (1991). Factors promoting acute and chronic diseases caused by yersiniae. Clin. Microbiol. Rev. *4*, 309–324.

Cingolani, P., Platts, A., Wang, L., Coon, M., Nguyen, T., Wang, L., Land, S.J., Lu, X., and Ruden, D.M. (2012). A program for annotating and predicting the effects of single nucleotide polymorphisms, SnpEff: SNPs in the genome of Drosophila melanogaster strain w1118; iso-2; iso-3. Fly (Austin) *6*, 80–92.

Cui, Y., Yu, C., Yan, Y., Li, D., Li, Y., Jombart, T., Weinert, L.A., Wang, Z., Guo, Z., Xu, L., et al. (2013). Historical variations in mutation rate in an epidemic pathogen, Yersinia pestis. Proc. Natl. Acad. Sci. USA *110*, 577–582.

Damgaard, P.B., Marchi, N., Rasmussen, S., Peyrot, M., Renaud, G., Korneliussen, T., Moreno-Mayar, J.V., Pedersen, M.W., Goldberg, A., Usmanova, E., et al. (2018). 137 ancient human genomes from across the Eurasian steppes. Nature *557*, 369–374.

Demeure, C.E., Dussurget, O., Mas Fiol, G., Le Guern, A.S., Savin, C., and Pizarro-Cerdá, J. (2019). Yersinia pestis and plague: an updated view on evolution, virulence determinants, immune subversion, vaccination, and diagnostics. Genes Immun. *20*, 357–370.

Eppinger, M., Worsham, P.L., Nikolich, M.P., Riley, D.R., Sebastian, Y., Mou, S., Achtman, M., Lindler, L.E., and Ravel, J. (2010). Genome sequence of the deep-rooted Yersinia pestis strain Angola reveals new insights into the evolution and pangenome of the plague bacterium. J. Bacteriol. *192*, 1685–1699.

Eroshenko, G.A., Nosov, N.Y., Krasnov, Y.M., Oglodin, Y.G., Kukleva, L.M., Guseva, N.P., Kuznetsov, A.A., Abdikarimov, S.T., Dzhaparova, A.K., and Kutyrev, V.V. (2017). Yersinia pestis strains of ancient phylogenetic branch 0.ANT are widely spread in the high-mountain plague foci of Kyrgyzstan. PLoS ONE *12*, e0187230.

Feldman, M., Harbeck, M., Keller, M., Spyrou, M.A., Rott, A., Trautmann, B., Scholz, H.C., Päffgen, B., Peters, J., McCormick, M., et al. (2016). A High-Coverage Yersinia pestis Genome from a Sixth-Century Justinianic Plague Victim. Mol. Biol. Evol. *33*, 2911–2923.

Gaydos, J.K., Zabek, E., and Raverty, S. (2009). Yersinia pseudotuberculosis septicemia in a beaver from Washington State. J. Wildl. Dis. *45*, 1182–1186.

Grewingk, C. (1878). Der Kauler- und der Rinne-Kaln am Burtnecksee in Livland. Neunzigste Sitzung der Dorpater Naturforscher-Gesellschaft am 28. Januar 1876. Sitzungsberichte Dorpater Naturforscher-Gesellschaft *4*, 206–225.

Herbig, A., Maixner, F., Bos, K.I., Zink, A., Krause, J., and Huson, D.H. (2016). MALT: Fast alignment and analysis of metagenomic DNA sequence data applied to the Tyrolean Iceman. BioRxiv. https://doi.org/10.1101/050559.

Huelsenbeck, J.P., and Ronquist, F. (2001). MRBAYES: Bayesian inference of phylogenetic trees. Bioinformatics *17*, 754–755.

Immel, A., Ţerna, S., Simalcsik, A., Susat, J., Šarov, O., Sîrbu, G., Hofmann, R., Müller, J., Nebel, A., and Krause-Kyora, B. (2020). Gene-flow from steppe individuals into Cucuteni-Trypillia associated populations indicates long-standing contacts and gradual admixture. Sci. Rep. *10*, 4253.

Jónsson, H., Ginolhac, A., Schubert, M., Johnson, P.L.F., and Orlando, L. (2013). MapDamage2.0: fast approximate Bayesian estimates of ancient DNA damage parameters. Bioinformatics *29*, 1682–1684.

Keller, M., Spyrou, M.A., Scheib, C.L., Neumann, G.U., Kröpelin, A., Haas-Gebhard, B., Päffgen, B., Haberstroh, J., Ribera I Lacomba, A., Raynaud, C., et al. (2019). Ancient *Yersinia pestis* genomes from across Western Europe reveal early diversification during the First Pandemic (541-750). Proc. Natl. Acad. Sci. USA *116*, 12363–12372.

Kislichkina, A.A., Bogun, A.G., Kadnikova, L.A., Maiskaya, N.V., Platonov, M.E., Anisimov, N.V., Galkina, E.V., Dentovskaya, S.V., and Anisimov, A.P. (2015). Nineteen Whole-Genome Assemblies of Yersinia pestis subsp. microtus, Including Representatives of Biovars caucasica, talassica, hissarica, altaica, xilingolensis, and ulegeica. Genome Announc. *3*, e01342-15.

Kislichkina, A.A., Bogun, A.G., Kadnikova, L.A., Maiskaya, N.V., Solomentsev, V.I., Platonov, M.E., Dentovskaya, S.V., and Anisimov, A.P. (2017). Eight whole-genome assemblies of Yersinia pestis subsp. microtus bv. caucasica isolated from the common vole (Microtus arvalis) plague focus in Dagestan, Russia. Genome Announc. *5*, e00847-17.

Kislichkina, A.A., Bogun, A.G., Kadnikova, L.A., Maiskaya, N.V., Solomentsev, V.I., Dentovskaya, S.V., Balakhonov, S.V., and Anisimov, A.P. (2018a). Nine whole genome assemblies of *Yersinia pestis* subsp. microtus bv. Altaica strains isolated from the Altai Mountain natural plague focus (no. 36) in Russia. Genome Announc. *6*, e01440-17.

Kislichkina, A.A., Bogun, A.G., Kadnikova, L.A., Maiskaya, N.V., Solomentsev, V.I., Sizova, A.A., Dentovskaya, S.V., Balakhonov, S.V., and Anisimov, A.P. (2018b). Six whole-genome assemblies of Yersinia pestis subsp. microtus bv. ulegeica (phylogroup 0.PE5) strains isolated from Mongolian natural plague foci. Genome Announc. *6*, e00536-18.

Krause-Kyora, B., Nutsua, M., Boehme, L., Pierini, F., Pedersen, D.D., Kornell, S.C., Drichel, D., Bonazzi, M., Möbus, L., Tarp, P., et al. (2018a). Ancient DNA study reveals HLA susceptibility locus for leprosy in medieval Europeans. Nat. Commun. *9*, 1569.

Krause-Kyora, B., Susat, J., Key, F.M., Kühnert, D., Bosse, E., Immel, A., Rinne, C., Kornell, S.C., Yepes, D., Franzenburg, S., et al. (2018b). Neolithic and medieval virus genomes reveal complex evolution of hepatitis B. eLife *7*, e36666.

Kriiska, A. (2015). Foreign materials and artefacts in the 4th and 3rd millennia BCE Estonian Comb Ware Complex. In When Gods Spoke. Researches and Reflections on Religious Phenomena and Artefacts. Studia in Honorem Tarmo Kulmar, P. Espak, M. Läänemets, and V. Sazonov, eds. (Tartu University Press), pp. 107–124.

Kutyrev, V.V., Eroshenko, G.A., Motin, V.L., Nosov, N.Y., Krasnov, J.M., Kukleva, L.M., Nikiforov, K.A., Al'khova, Z.V., Oglodin, E.G., and Guseva, N.P. (2018). Phylogeny and classification of Yersinia pestis through the lens of strains from the Plague Foci of commonwealth of independent states. Front. Microbiol. *9*, 1106.

Li, H., and Durbin, R. (2009). Fast and accurate short read alignment with Burrows-Wheeler transform. Bioinformatics *25*, 1754–1760.

Loze, I. (2001). Some aspects of research on Middle Neolithic amber in the Lake Lubāns depression. In Baltic Amber: Proceedings of the International Interdisciplinary Conference. Baltic Amber in Natural Sciences, Archaeology and Applied Arts: 13-18 September 2001, Vilnius., Palana., Nida., and A. Butrimas, eds. (Vilniaus Dailes Akademijos Leidykla), pp. 125–133.

Lübke, H., Brinker, U., Meadows, J., and Bērziņš, V. (2016). New research on the human burials of Riņņukalns, Latvia. In Mesolithic Burials–Rites, Symbols and Social Organization of Early Postglacial Communities, J. Grünberg, B. Gramsch, L. Larsson, J. Orschiedt, and H. Meller, eds. (Verlag Beier & Beran), pp. 241–256.

Mathieson, I., Alpaslan-Roodenberg, S., Posth, C., Szécsényi-Nagy, A., Rohland, N., Mallick, S., Olalde, I., Broomandkhoshbacht, N., Candilio, F., Cheronet, O., et al. (2018). The genomic history of southeastern Europe. Nature *555*, 197–203.

McKenna, A., Hanna, M., Banks, E., Sivachenko, A., Cibulskis, K., Kernytsky, A., Garimella, K., Altshuler, D., Gabriel, S., Daly, M., and DePristo, M.A. (2010). The Genome Analysis Toolkit: a MapReduce framework for analyzing next-generation DNA sequencing data. Genome Res. *20*, 1297–1303.

Meadows, J., Bērziņš, V., Legzdiņa, D., Lübke, H., Schmölcke, U., Zagorska, I., and Zariņa, G. (2018). Stone-age subsistence strategies at Lake Burtnieks, Latvia. J. Archaeol. Sci. Rep. *17*, 992–1006.

Núñez, M., and Franzén, P. (2011). Implications of Baltic amber finds in northern Finland 4000–2000 BCE. Archaeologia Lituana *12*, 10–24.

Parkhill, J., Wren, B.W., Thomson, N.R., Titball, R.W., Holden, M.T., Prentice, M.B., Sebaihia, M., James, K.D., Churcher, C., Mungall, K.L., et al. (2001). Genome sequence of Yersinia pestis, the causative agent of plague. Nature *413*, 523–527.

Peltzer, A., Jäger, G., Herbig, A., Seitz, A., Kniep, C., Krause, J., and Nieselt, K. (2016). EAGER: efficient ancient genome reconstruction. Genome Biol. *17*, 60.

Rambaut, A., Lam, T.T., Max Carvalho, L., and Pybus, O.G. (2016). Exploring the temporal structure of heterochronous sequences using TempEst (formerly Path-O-Gen). Virus Evol. *2*, vew007.

Rambaut, A., Drummond, A.J., Xie, D., Baele, G., and Suchard, M.A. (2018). Posterior summarization in Bayesian phylogenetics using Tracer 1.7. Syst. Biol. *67*, 901–904.

Rascovan, N., Sjögren, K.G., Kristiansen, K., Nielsen, R., Willerslev, E., Desnues, C., and Rasmussen, S. (2019). Emergence and Spread of Basal Lineages of Yersinia pestis during the Neolithic Decline. Cell *176*, 295–305.e10.

Rasmussen, S., Allentoft, M.E., Nielsen, K., Orlando, L., Sikora, M., Sjögren, K.G., Pedersen, A.G., Schubert, M., Van Dam, A., Kapel, C.M.O., et al. (2015). Early divergent strains of Yersinia pestis in Eurasia 5,000 years ago. Cell *163*, 571–582.

Rohland, N., Harney, E., Mallick, S., Nordenfelt, S., and Reich, D. (2015). Partial uracil-DNA-glycosylase treatment for screening of ancient DNA. Philos. Trans. R. Soc. Lond. B Biol. Sci. *370*, 20130624.

Rütimeyer, L. (1877). Ueber die Thierreste des Rinnekalns. Sitzungsberichte Dorpater Naturforscher-Gesellschaft *4*, 534–539.

Sievers, C.G. (1875). Ein normannisches Schiffsgrab bei Ronneburg und die Ausgrabung des Rinnehügels. Sitzung vom 18. Oktober 1875. Verhandlungen der Berliner Gesellschaft für Anthropologie, Ethnologie und Urgeschichte 1875. Z. Ethnol. *7*, 214–223.

Spyrou, M.A., Tukhbatova, R.I., Feldman, M., Drath, J., Kacki, S., Beltrán de Heredia, J., Arnold, S., Sitdikov, A.G., Castex, D., Wahl, J., et al. (2016). Historical Y. pestis Genomes Reveal the European Black Death as the Source of Ancient and Modern Plague Pandemics. Cell Host Microbe *19*, 874–881.

Spyrou, M.A., Tukhbatova, R.I., Wang, C.C., Valtueña, A.A., Lankapalli, A.K., Kondrashin, V.V., Tsybin, V.A., Khokhlov, A., Kühnert, D., Herbig, A., et al. (2018). Analysis of 3800-year-old Yersinia pestis genomes suggests Bronze Age origin for bubonic plague. Nat. Commun. *9*, 2234.

Spyrou, M.A., Keller, M., Tukhbatova, R.I., Scheib, C.L., Nelson, E.A., Andrades Valtueña, A., Neumann, G.U., Walker, D., Alterauge, A., Carty, N., et al. (2019). Phylogeography of the second plague pandemic revealed through analysis of historical Yersinia pestis genomes. Nat. Commun. *10*, 4470.

Stamatakis, A. (2014). RAxML version 8: a tool for phylogenetic analysis and post-analysis of large phylogenies. Bioinformatics *30*, 1312–1313.

Susat, J., Bonczarowska, J.H., Pētersone-Gordina, E., Immel, A., Nebel, A., Gerhards, G., and Krause-Kyora, B. (2020). Yersinia pestis strains from Latvia show depletion of the pla virulence gene at the end of the second plague pandemic. Sci. Rep. *10*, 14628.

Virchow, R. (1877). Bericht über eine archäologische Reise nach Livland. Sitzung vom 20. October 1877. Verhandlungen der Berliner Gesellschaft für Anthropologie, Ethnologie und Urgeschichte 1877. Z. Ethnol. *9*, 365–437.

Wagner, D.M., Klunk, J., Harbeck, M., Devault, A., Waglechner, N., Sahl, J.W., Enk, J., Birdsell, D.N., Kuch, M., Lumibao, C., et al. (2014). Yersinia pestis and the plague of Justinian 541-543 AD: a genomic analysis. Lancet Infect. Dis. *14*, 319–326.

Wen, B., Wang, X., and Zhang, B. (2019). PepQuery enables fast, accurate, and convenient proteomic validation of novel genomic alterations. Genome Res. *29*, 485–493.

Zhgenti, E., Johnson, S.L., Davenport, K.W., Chanturia, G., Daligault, H.E., Chain, P.S., and Nikolich, M.P. (2015). Genome assemblies for 11 Yersinia pestis strains isolated in the Caucasus region. Genome Announc. *3*, e01030-15.

Zimbler, D.L., Schroeder, J.A., Eddy, J.L., and Lathem, W.W. (2015). Early emergence of Yersinia pestis as a severe respiratory pathogen. Nat. Commun. *6*, 7487.

STAR★METHODS

KEY RESOURCES TABLE

REAGENT or RESOURCE	SOURCE	IDENTIFIER
Biological samples		
Human archaeological remains	This study	ENA: PRJEB42185, https://www.ebi.ac.uk/ena/browser/view/PRJEB42185
Software and algorithms		
Clip and Merge v1.7.7	Peltzer et al., 2016	https://github.com/apeltzer/ClipAndMerge
MALT v0.4.1	Herbig et al., 2016	https://software-ab.informatik.uni-tuebingen.de/download/malt/welcome.html
BWA v0.7.15	Li and Durbin, 2009	https://sourceforge.net/projects/bio-bwa/files/
MapDamage v2	Jónsson et al., 2013	https://ginolhac.github.io/mapDamage/
GATK v3.4-0-g7e26428	McKenna et al., 2010	https://github.com/broadinstitute/gatk/releases
MulitiVCFAnalyzer v0.85.1	Bos et al., 2014	https://github.com/alexherbig/MultiVCFAnalyzer/releases
RAxML v8.2.12	Stamatakis, 2014	https://github.com/stamatak/standard-RAxML
MrBayes v3.2.7a	Huelsenbeck and Ronquist, 2001	https://github.com/NBISweden/MrBayes/tree/v3.2.7a
TempEst v1.5.3	Rambaut et al., 2016	http://tree.bio.ed.ac.uk/software/tempest/
BEAST2 v2.6	Bouckaert et al., 2019	https://www.beast2.org/
Tracer v1.7.1	Rambaut et al., 2018	https://www.beast2.org/tracer-2/
SnpEFF v3.1	Cingolani et al., 2012	https://pcingola.github.io/SnpEff/download/
Proteome Discoverer software 2.2.0.388	Thermo Fischer	https://www.thermofisher.com/us/en/home/industrial/mass-spectrometry/liquid-chromatography-mass-spectrometry-lc-ms/lc-ms-software/multi-omics-data-analysis/proteome-discoverer-software.html
Deposited data		
RV2039 *Y.pestis* aDNA data	This study	ENA: PRJEB42185, https://www.ebi.ac.uk/ena/browser/view/PRJEB42185

RESOURCE AVAILABILITY

Lead contact

Further information and requests for resources and reagents should be directed to and will be fulfilled by the lead contact, Ben Krause-Kyora (b.krause-kyora@ikmb.uni-kiel.de).

Materials availability

This study did not generate new unique reagents.

Data and code availability

The datasets generated during this study are available at the European Nucleotide Archive under the accession PRJEB42185.

EXPERIMENTAL MODEL AND SUBJECT DETAILS

Anthropological Rudolf Virchow Collection

This collection of prehistorical and historical human skulls, which Rudolf Virchow (RV) started to assemble in 1870, is preserved today by the BGAEU. BGEAU-RV 1852 and BGEAU-RV 2039 are the official collection labels of the samples investigated in this study, hereafter referred to as RV 1852 and RV 2039.

METHOD DETAILS

Anthropological analysis

The human remains were examined according to standard osteological methods (Brinker et al., 2018). For the genetic analyses, both petrous bones and teeth were collected for the individuals RV 1852 and 2017/1; for 2018/1 a petrous bone and for RV 2039 a tooth were sampled.

aDNA extraction and sequencing

All lab work was carried out in a dedicated aDNA facility. DNA extraction from bone/tooth powder, double-stranded half-UDG library preparation with unique index combinations for each sample and sequencing (Illumina HiSeq4000 (2x75bp)) were performed following established protocols (Krause-Kyora et al., 2018a; Rohland et al., 2015). The generated sequences were pre-processed (adaptor clipping, merging, and trimming) using the software Clip and Merge with default parameters (Peltzer et al., 2016).

Yersinia pestis genetic analyses

Using the software MALT with the parameters described in Krause-Kyora et al. (2018b) and Susat et al. (2020), all samples were screened for the presence of viral and bacterial pathogens (Herbig et al., 2016). The reads of the *Y. pestis*-positive sample RV 2039 were subsequently mapped to the *Y. pestis* genome and its three plasmids (NC_0031431.1; NC_003131.1; NC_003134.1; NC_003132.1) with BWA (Li and Durbin, 2009). MapDamage 2.0 was used to rescale the terminal damage that remained after the half-UDG library preparation (Jónsson et al., 2013). The subsequent generation of VCF files was done as described in Susat et al. (2020; Table S1). VCFs were generated for RV 2039, one *Y. pseudotuberculosis* strain and 276 other *Y. pestis* strains (Bos et al., 2011, 2016; Cui et al., 2013; Damgaard et al., 2018; Eppinger et al., 2010; Eroshenko et al., 2017; Feldman et al., 2016; Keller et al., 2019; Kislichkina et al., 2015, 2017, 2018a, 2018b; Kutyrev et al., 2018; Parkhill et al., 2001; Spyrou et al., 2016, 2019; Zhgenti et al., 2015). The MulitiVCFAnalyzer was used to generate an alignment containing only phylogenetically informative positions with at least 3x coverage and an allele support of at least 90% of the sequences (Bos et al., 2014). To improve visual resolution, variants specific to *Y. pseudotuberculosis* were filtered from the resulting file which was then used for phylogenetic analysis. RAxML was executed with the GTRGAMMA model and 1,000 bootstraps (Stamatakis, 2014). MrBayes was executed with the GTR model and 5,000,000 generations (Huelsenbeck and Ronquist, 2001).

Molecular dating

A subset of 41 representative *Y. pestis* genomes and RV 2039 were used to generate a SNP-based alignment with the MultiVCF-Analyzer (Table S1; Rascovan et al., 2019; Susat et al., 2020). Based on this alignment, we calculated a rooted maximum likelihood (ML) tree with RAxML and 100 bootstraps and used TempEst for verification of a temporal signal (correlation coefficient 0.57 (R2 = 0.32) (Rambaut et al., 2016). R was used to plot the TempEst data and calculate the 95% confidence interval (Figure S1). The resulting tree was utilized as a starting tree for BEAST2 version 2.6 (Bouckaert et al., 2019). Dating analysis followed previous work using an uncorrelated relaxed clock with lognormal distribution and the GTR+G4 substitution model (Bouckaert et al., 2019; Rascovan et al., 2019). Furthermore, a coalescent constant population size was assumed. The dates published for previous historical *Y. pestis* genomes were transformed to BP by setting the year 1950 as age 0 (with the mean as the age and the boundaries as an interval for a prior uniform distribution). Two different runs were executed in BEAST2. One run in which the RAxML starting tree was provided and BEAST2 was allowed to alter the tree, and another in which no starting tree was provided. Multiple versions from the same run were combined and post burn-in data were visualized using Tracer version 1.7.1 (Rambaut et al., 2018). All effective sample size (ESS) values were at least greater than 250 (Figure S2). LogCombiner and TreeAnnotator from BEAST2 were used to combine the result files and to generate maximum clade credibility trees.

SNP effect and analysis of virulence factors

The v*cf.* file was used by SnpEFF for the annotation of SNPs (Cingolani et al., 2012). RV 2039 had 106 unique SNPs with a coverage >3x and a support of 80% of the reads (Table S2). Coverage of virulence genes was calculated and plotted using Gnuplot version 5.2.

Human population genetic analyses

Mapping of reads, SNP genotyping, genetic sex determination, contamination estimation, principal component analysis, ADMIXTURE, f3 outgroup statistics and qpADM were conducted as described previously (Immel et al., 2020; Figure S4).

Proteomic analysis

Sample preparation for bottom-up LC-MS/MS analysis

After adding 500 μL of 0.5 M EDTA in MilliQ water, the powdered tooth sample (50 mg) was homogenized with a pellet pestle and incubated overnight at 20°C to demineralize the bone matrix and extract the proteins. The sample was then centrifuged for 5 minutes at 20°C and 14000 g to collect the supernatant (EDTA-fraction) which was stored on ice. The pellet was resuspended in 300 μL of a

lysis buffer (4% SDS, 0.1 M dithiothreitol (DTT), 0.1 M Tris-HCl), homogenized with a pellet pestle and incubated for 10 minutes at 95°C for further demineralization and reduction. Subsequently, the sample was cooled down and centrifuged for 5 minutes at 20°C and 14000 g to collect the supernatant (SDS-fraction).

To reduce the disulfide bonds (EDTA and SDS-fraction), 75 μL of a reduction buffer (0.2 M DTT in 50 mM ammonium bicarbonate (ABC), 5% acetonitrile (ACN)) was added and incubated for 30 minutes at 60°C, and the sample was cooled down prior to alkylation. For alkylation, both fractions were incubated for 20 minutes in the dark with 75 μL 0.8 M iodoacetamide-solution (IAA) in 50 mM ABC, 5% ACN.

Tryptic digestion was performed using the single-pot, solid phase enhanced sample preparation (SP3) protocol. The bead stock was prepared by adding 110 μL hydrophilic to the same number of hydrophobic beads which are delivered in 0.05% azide solution. After washing three times with 1.1 mL MilliQ water and collecting the beads with the help of magnets, 550 μL MilliQ water was added to obtain a final bead concentration of 20 mg/ml. 750 μL of ethanol (96%) and 50 μL of the bead solution were added to the EDTA-fraction and 450 μL of ethanol (96%) and 50 μL of the bead solution were added to the SDS-fraction. Both were gently mixed by swinging lightly and incubated for 18 minutes at room temperature. The supernatant was then removed carefully with a magnet and the samples were washed 3 times with 150 μL 80% ethanol to remove contaminants and salts from the previous steps. 150 μL digestion buffer (50 mM ABC) and 10 μL of 40 ng/μl trypsin (sequencing grade, Promega) was added. Digestion took place overnight at 37°C. The supernatant was collected with the help of a magnet and the peptide solution was cleaned with home-made C18 stage tips. The stage tips were conditioned first with 150 μL methanol, second with 150 μL 80% ACN, 0.5% acetic acid and third with 150 μL 0.5% acetic acid. Subsequently, the samples were loaded on the stage tips and washed with 150 μL 0.5% acetic acid. The elution took place by first adding 40 μL 40% ACN, 0.5% acetic acid, 40 μL 60% ACN, 0.5% acetic acid and two times with 40 μL 80% ACN, 0.5% acetic acid. The samples were dried in a Speed Vac and stored at −20°C.

LC-MS/MS analysis

The samples were resuspended in 15 μL loading buffer (3% ACN, 0.1% TFA). Chromatographic separation was performed on an Ultimate 3000 UHPLC system (Thermo, Dreieich, Germany) equipped with an Acclaim PepMap C18 2UM 75UMx500MM NV FS column (Thermo, Dreieich, Germany) coupled online to a mass spectrometer. The following eluents were used A: 0.05% formic acid and B: 80% ACN, 0.04% formic acid. Initial chromatographic conditions were isocratic 4% B for 2 minutes followed by different gradients for the EDTA- and SDS-fractions, respectively, as the peaks in the EDTA run elute later than the peaks in the SDS run.

EDTA-fraction: from minute 2 to 92 (eluent B 5% to 50%), from minute 92 to 97 (eluent B 50% to 95%), from minute 97 to 107 (eluent B 95%) and from minute 107 to 120 (eluent B 5%).

SDS-fraction: from minute 2 to 30 (eluent B 10% to 30%), from minute 30 to 92 (eluent B 30% to 55%) and from minute 92 to 97 (eluent B 55% to 95%).

A constant flow rate of 300 nL / minute was used and 5 μL of the sample was injected per run.

LC-separation was coupled online to an Orbitrap Fusion Lumos mass spectrometer (Thermo, Dreieich, Germany) utilizing HCD ion activation at a collision energy of 30%. A full scan MS acquisition was performed (resolution 120000) with subsequent data dependent MS/MS (resolution 30000) with a cycle time of 3 s. The MS data files were searched against a set of FASTA-databases containing human proteins (Uniprot download 2019/03/13), *Y. pestis* proteins (Uniprot download 2019/03/14) and a cRAP list of common laboratory contaminants. The searches were performed using the Proteome Discoverer software (Version 2.2.0.388) and the SequestHT search algorithm. A false discovery rate (FDR) for peptides and proteins from 0.01 (strict) to 0.05 (relaxed) was applied. A maximum of two missed cleavage sites, a precursor mass tolerance of 10 ppm and a fragment mass tolerance of 0.02 Da were allowed. Dynamic modifications: oxidation (M, P); deamidation (N, Q). Static Modification: Carbamidomethylation (C). Identified peptides were additionally interrogated with the PepQuery-algorithm (Wen et al., 2019).